arXiv:cond-mat/0506278v1 [cond-mat.stat-mech] 13 Jun 2005

A self-adjusted Monte Carlo simulation as a model for financial markets with central regulation

Denis Horváth *, Martin Gmitra, Zoltán Kuscsik

Institute of Physics, Šafárik University, Park Angelinum 9, 040 01 Košice, Slovak Republic

Abstract

Properties of the self-adjusted Monte Carlo algorithm applied to 2d Ising ferromagnet are studied numerically. The endogenous feedback form expressed in terms of the instant running averages is suggested in order to generate a biased random walk of the temperature that converges to criticality without an external tuning. The robustness of a stationary regime with respect to partial accessibility of the information is demonstrated. Several statistical and scaling aspects have been identified which allow to establish an alternative spin lattice model of the financial market. It turns out that our model alike model suggested by S. Bornholdt, Int. J. Mod. Phys. C **12** (2001) 667, may be described by Lévy-type stationary distribution of feedback variations with unique exponent $\alpha_1 \sim 3.3$. However, the differences reflected by Hurst exponents suggest that resemblances between the studied models seem to be nontrivial.

Key words: Monte Carlo, self-adjusted parameters, econophysics, portfolio diversification, Lévy distribution
PACS: : 02.70.Uu, 05.50.+q, 89.65.Gh, 05.65.+b

1 Introduction

During the past decades, the financial markets around the world have become more and more interconnected. The financial globalization has changed the organization structure of the stock markets by creating new risks and challenges for market participants. Dramatic expansion of the cross-border financial flows

* Corresponding author.
Email address: horvath.denis@gmail.com (Denis Horváth).

as well as domestic flows within the countries due to very rapid increase of telecommunication and computer-based products have emerged. As a consequence, the world financial markets are increasingly efficient today than ever before.

The integration and globalization process opens discussion about the activity of the central economic institutions that focus attention to financial market monitoring. The subsequent regulatory legislative yields asymptotically to dynamic balance between coalitions based on agreements of the cooperating companies and on the other hand competitors that enhance a diversity of the price trends. The *feedback* signals of different reliability are monitored and daily evaluated by central economic institutions. Consequently, this affects correlated decisions of the market participants. An expected effect of the global self-regulation is a portfolio efficiency.

Recently, there have been many attempts to gain a control over the dynamics of complex systems. The approaches based on the principles of feedback and adaptivity emerges as a perspective branch (1). The importance of the positive feedback mechanism in the economic context has been studied in Ref. (2). An approach based on the feedback control of spatially extended optical system has been employed in the Ref. (3). The feedback mechanism is also exploited in Monte Carlo (MC) algorithm introduced by us recently in Ref. (4). The algorithm is formulated as a random walk of temperature variable biased by feedback that mixes current and past stochastic signals, originating at the platform of extended statistical system. The time integrated signals are used to build up the actions shifting an instant temperature towards the critical temperature value. Due to limited memory depth, the convergence process is necessarily accompanied by uncertainty. Since the feedback treats a partial information only, many parallels with risky decisions within the business world can be found. Therefore, the MC feedback model may be used for simulation of decision-making in the stochastic environment.

The plan of the paper is as follows. In the next section the self-adjusted MC algorithm is reintroduced briefly. Its relationship to non-equilibrium spin updates is discussed in Sec. 3. The Sec. 4 deals with the statistics of spin clusters near the critical conditions and the self-adjusted algorithm is related to cellular automaton models of self-organized criticality (SOC). In Sec. 5, the applications of mentioned MC dynamics to models of financial markets is presented.

2 The self-adjusted random walk near criticality

Before proceeding to the introduction of financial model, we recall the salient points of the self-adjusted MC model (4) that is based on the random walk of

the temperature variable T_t defined by the one-step recurrence

$$T_{t+1} = T_t + \xi_t \Delta \, \mathrm{sign}(F_t) \, , \tag{1}$$

where Δ parameterizes a maximum step length $|T_{t+1} - T_t|$, randomized by ξ_t that is uniformly distributed within the $\langle -1, 1 \rangle$ range. The subscript t accounts for MC steps per N degrees of freedom. The *feedback regulatory response*

$$F_t = \frac{\langle E^3 \rangle_t - 3\langle E \rangle_t \langle E^2 \rangle_t + 2\langle E \rangle_t^3}{T_t^4 N} - 2\frac{\langle E^2 \rangle_t - \langle E \rangle_t^2}{T_t^3 N} \, , \tag{2}$$

mixes an influence of bias and randomness involved in the energy series $\{E_t\}$ that represents outcome of some extended statistical system. Eq.(2) approximates a temperature derivative of the specific heat $\frac{\partial}{\partial T}[(\, \langle E^2 \rangle_{\mathrm{eq}} - \langle E \rangle_{\mathrm{eq}}^2 \,)/(T^2 \, N)]$ at the canonical equilibrium (eq) ensemble defined by the constant temperature $T \sim T_t$ (5). In Eq.(2) the canonical averages are approximated by instantaneous running averages of the energy cumulants $\langle E^p \rangle_t, \;\; p = 1, 2$ calculated with the assistance of linear filter (6) as it follows

$$\langle E^p \rangle_t = (1 - \eta) \langle E^p \rangle_{t-1} + \eta E_t^p \; . \tag{3}$$

Here the plasticity parameter $\eta \in (0, 1)$ reweights an energy samples E_t according to delay. For $\eta \to 0$, running averages vary slowly and long-memory processes dominates, whereas in the limit $\eta \to 1^-$ the memorizing becomes faster but less efficient.

The feedback is applied to maintain the critical regime of the 2d Ising spin micromodel of ferromagnet. This is defined for $i = 1, 2, \ldots, N = L^2$ sites of $L \times L$ square lattice characterized by the exchange energy $E = -\sum_{\mathrm{nn}} S_i S_j$, $S_i \in \{-\frac{1}{2}, \frac{1}{2}\}$, where exchange coupling constant rescales an instant temperature T_t. The nearest neighbor (nn) interaction is considered. This interaction picture is supplemented by the periodic boundary conditions in all directions. The standard Metropolis single-spin-flip algorithm (5; 7) where two states are linked by the flip acceptance probability $p_{\mathrm{acc}} = \min\{1, \exp\left(-\delta E_i / T_t\right)\}$ depends on the energy change δE_i at ith site. The technical issue of the proposed implementation is that T_t is hold constant during $N = L^2$ spin updates (i.e. 1 MC step per sample). The example which illustrates T_t dynamics is shown in Fig.1. As follows from Eq.(3), a filtered information serves to provide T_{t+1} near criticality. In compliance with a previous facts, the *feedback role* in dynamics can be summarized as follows: a) it *receives* series of energy $\{E_t\}$ values from extended statistical system (or only sufficient part of the series is served for this purpose); b) it *treats* the series via the linear *filtering* that generates *running averages* $\langle E^p \rangle_t$; c) it transmits the *regulatory signals* $\mathrm{sign}(F_t)$ via the temperature given by Eq.(1).

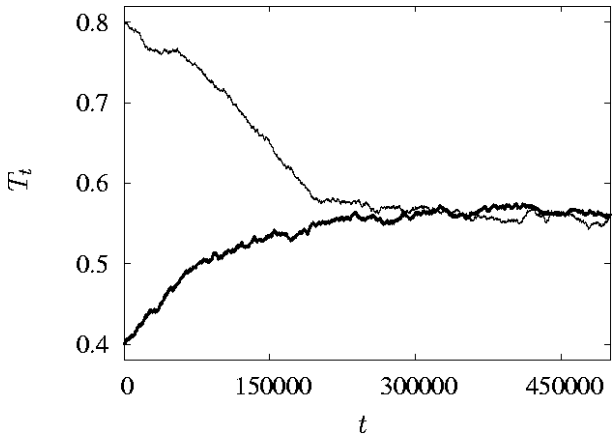

Fig. 1. Temporal dependence of self-adjusted MC model for transient T_t dynamics obtained for $L = 90$ and parameters $\eta = 0.01$, $\Delta = 10^{-5}$. Two paths [starting from $T_{t=0} = 0.4$, and 0.8] tend to the unique attractor $T_{\rm c}(L)$ (asymptotic regime), as the variable t increases.

After the transient time the thermal noise overcomes a regular bias involved in stochastic F_t and system with feedback maintain a stationary regime. Due to fluctuations of T_t a non-equilibrium distribution is generated. Therefore, the expectation mean values, worth our interest are given by

$$\langle\, T^p \,\rangle = \frac{1}{n_1 - n_0} \sum_{t'=n_0}^{n_1} T_{t'}^p \;, \qquad p = 1, 2\,. \tag{4}$$

where $n_1 \gg n_0$. If the number of excluded steps n_0 is larger than the transient time, the average $\langle T \rangle$ estimates critical point of the extended system. Thus, the observation time is defined by $\tau_{\rm obs} = n_1 - n_0$. In our simulations we used $n_0 \simeq 10^5$, $n_1 \simeq 10^7$.

3 The finite-size effects of $\langle T \rangle$

There are many examples of the simple non-equilibrium spin-flip stochastic models (8; 9) giving rise to the various dynamical phases. To simulate nearly equilibrium systems, the specific non-equilibrium approaches have been suggested. For instance, the Ref. (10) exploits the controlled growth of percolating spin cluster.

The postulation of artificial dynamics clearly places novel time scales into original equilibrium problem. In our case the combination of two parameters η and Δ affect the distance between a stationary non-equilibrium statistics and canonical equilibrium. The basic properties of stationary non-equilibrium regime can be summarized as follows:

1. The stationary regime with a ferro-paramagnetic order and positive $\langle T\rangle$ is stabilized by a sufficiently slow dynamics limited to $\Delta < \Delta_{\rm tr}(\eta)$, where $\Delta_{\rm tr}(\eta)$ is a threshold value. The irreversible drop to negative $\langle T\rangle$ (antiferromagnetic order) occurs at $\Delta = \Delta_{\rm tr}$.

   Similar transition can be found for the coupled map lattice where antiferromagnetic order is generated spontaneously by ferromagnetic couplings accompanied by sufficiently fast synchronous dynamics (11). For $L = 10$, $\eta = 10^{-3}$ we estimated $\Delta_{\rm tr} \sim 2.2 \times 10^{-3}$.
2. The canonical equilibrium limit $\langle T\rangle \to T_{\rm c}(L)$, where $T_{\rm c}(L)$ is the pseudocritical temperature of specific heat, is reached for the sufficiently slow dynamics $1 \gg \Delta > 0$, when the feedback memory is deep ($1 \gg \eta$) and parameters admit the scale separation $\eta \gg \Delta$. In addition, the stationary averages have to be accumulated for $\tau_{\rm obs} \gg 1/\eta$.
3. For stationary regime (see point 1) the nonzero variance $\langle (T - \langle T\rangle)^2\rangle$ gives rise to the broad energy distribution in comparison to Boltzmann one.

The question of practical relevance is whether true $T_{\rm c}$ can be attained by non-equilibrium dynamics. The result of simulation realized for $\eta = 10^{-5}$, $\Delta = 10^{-9}$ is depicted in Fig.2. The standard finite-size dependence of $T_{\rm c}(L) \simeq \langle T\rangle = T_{\rm c} + b/L$ (5) (where b denotes the thermal coefficient) has been obtained from the fit. Without additional tuning the simulation provides estimate $T_{\rm c} \simeq 0.5679$ of the equilibrium exact value $T_{\rm c}^{\rm ex} \simeq [2\ln(1+\sqrt{2})]^{-1} \simeq 0.56729$ (12).

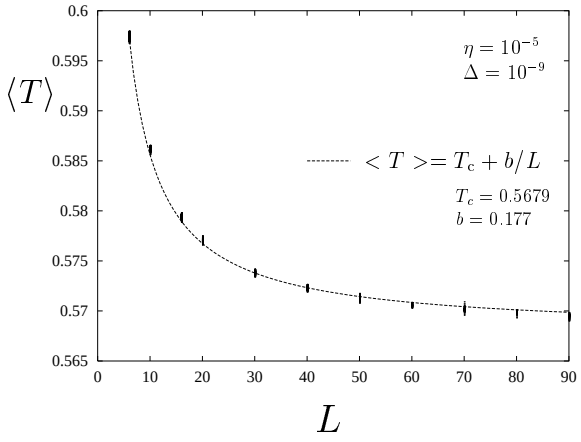

Fig. 2. The non-equilibrium dynamics confirms $1/L$ finite-size dependence of pseudo-critical temperature. True critical value $T_{\rm c}$ is estimated from the fit $\langle T\rangle = T_{\rm c} + b/L$ for $L = 10, 20, \ldots, 90$.

As one can see in Fig.3a follows that substantial finite-size corrections occur for a short-time memory. In that case, the temperature mean value can be interpolated by

$$\langle T\rangle = T_{\rm c} + \frac{b}{L} - A\eta^q\,, \qquad \Delta \ll \eta < \eta_{\rm c}(L)\,, \tag{5}$$

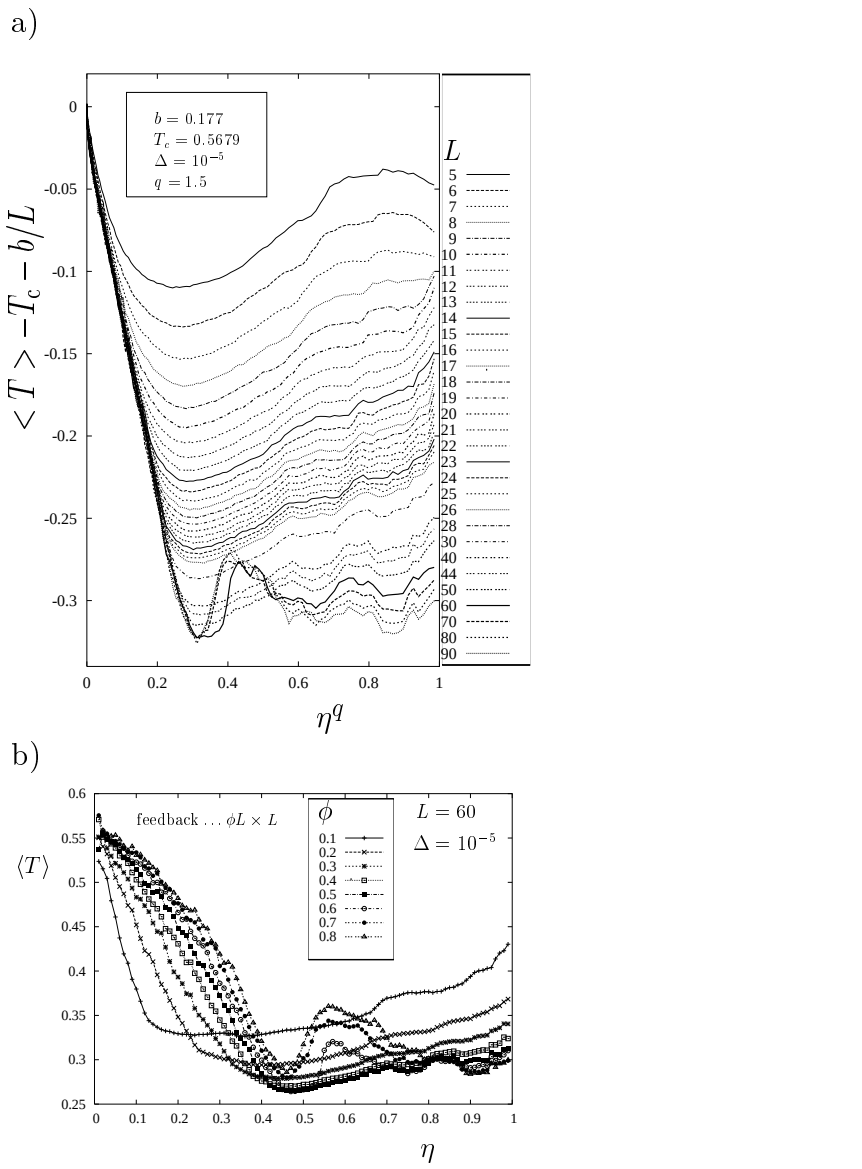

Fig. 3. a) The η-dependence of $\langle T \rangle$ calculated for $L = 5, 6, 7, 8, 9, \ldots, 70, 80, 90$ lattices. The mean temperature decreases with η for $\eta < \eta_c(L)$. The upper bound is chosen to guarantee that $\langle T \rangle$ calculated for different lattices merge to the unique η^q asymptotics. b) The robustness (or failure tolerance) of averages with respect to feedback that accumulates partial statistics for the rectangular segment $[\phi L] \times L$, $0 < \phi < 1$ of $L \times L$ lattice.

where cut-off $\eta_c(L)$ is roughly interpolatated by $\eta_c(L) = \eta_\infty - 0.343/L$ with $\eta_\infty = 0.468$. From the fit carried out within the range $\eta \in \langle\, 0,\, \frac{\eta_c}{2} \,\rangle$ we have determined the exponent $q \simeq 1.5$. Assuming that the lowest mean value $\langle T \rangle \sim T_{\min} \sim T_2(L)$, where η_∞ is achieved, for $L \to \infty$ we may write $A = (T_c - T_{\min})/\eta_\infty^q$. The presence of the temperature lower bound is associated with the condition that peak of specific heat is formed. This implies the requirement of a residual acceptance of single-spin-flips at very low temperatures. The bound

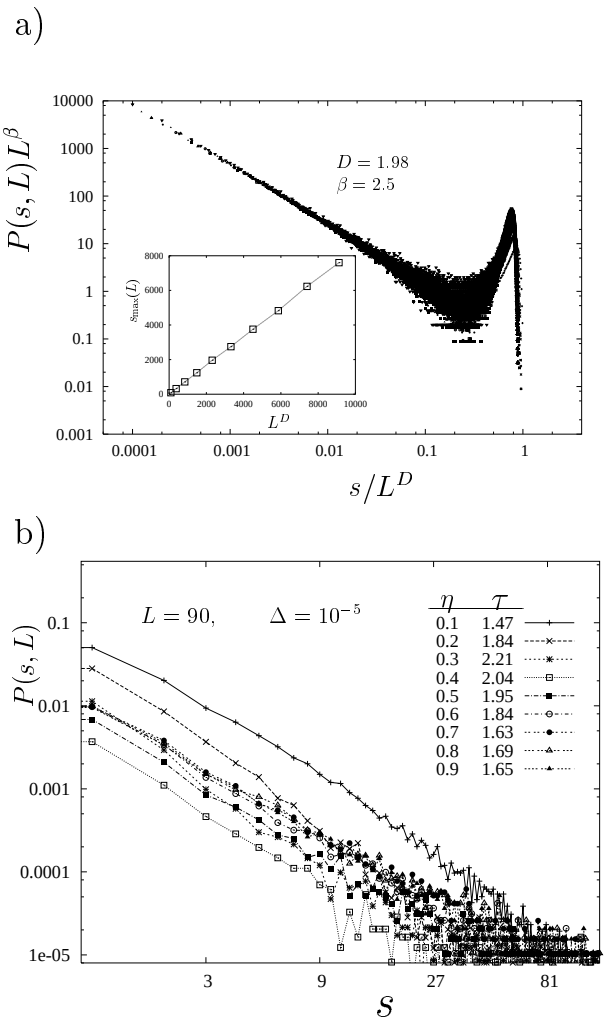

Fig. 4. a) The pdf's of spin cluster for $L = 10, \ldots, 100$. The inset shows a lattice size dependence of the peak position $s_{\max}(L) \propto L^D$. The simulation is carried out for parameters $\eta = 10^{-2}, \Delta = 10^{-5}$. b) A log-log plot of spin cluster size pdf considered for different η. The exponent τ obtained from the fit $P(s,L) \propto s^{-\tau}$ within the range $s < 30$. The differences in $\tau \in (1.47, 2.21)$ are connected with changes $\langle T \rangle$ (see Fig.3).

can be explained in the frame of two-level specific heat model denoted as C_2. The model takes into account only single branch of ground state $-L^2/2$ (since the ergodicity is broken, the ground state is counted once) and L^2-fold single-spin excitation of energy $2-L^2/2$. The condition for extreme $\mathrm{d}C_2/\mathrm{d}T|_{T=T_2} = 0$ yields equation $(T_2 - 1)\exp(2/T_2) + L^2(1 + T_2) = 0$. The last relation predicts a monotonous decrease of T_2 with L and solution can be simply approximated by $T_2 \sim \frac{1}{\ln L}$ for infinite L asymptotics. To estimate T_2 we have carried out simulation for $L = 90$ and $\eta \in (0.45, 0.55)$ that gives $\langle T \rangle$ from $(0.25, 0.3)$ range. The mean value $\langle T \rangle$ is approximated by $T_2 = 0.212 \sim \frac{1}{\ln(90)} = 0.222$.

The assumption about the energy gap corresponding to two lowest levels is

consistent with the presence of the crossing over memory depth $1/\eta_c \sim 2$ (two MC steps). To maintain a stationary regime the substantial memory reduction for $\eta > \eta_c$ have to be compensated by the enlarged $\langle T \rangle$ value. We observed that for $\eta \sim \eta_c$ the ergodic time τ_e between the plus and minus magnetization stages diverges as $\tau_e \propto L^z$, where $z \simeq 2$ is the dynamical exponent (13). If τ_{obs} is smaller than τ_e, the broken symmetry can be detected. Clearly, for $\eta > \eta_c$ the "jaggy" $\langle T \rangle(\eta)$ dependence indicates the occupancy of only few lowest energy levels.

4 The relationship to SOC and percolation models

The concept of SOC proposed by Bak (14) represents the unifying theoretical framework of systems that drive themselves spontaneously to critical regime. The sand pile, forest-fire (15) and game-of-life (16) are well-known examples of cellular automaton SOC models. Their stationary regime can be characterized by invariant *probability distribution functions* (pdf's) of spatial or temporal measures of the dissipative events called *avalanches*. The corresponding pdf's include a power-law intervals with the specific non-equilibrium critical exponents.

According to Ref. (17), the stationary SOC regime implies the operation of inherent feedback mechanism. On the contrary, our model has explicitely defined global feedback coupled to the MC dynamics. Such coupling is completely different from the standard models of SOC, but the arguments given in this section suggest that additional coupling anchors statistical properties indistinguishable from SOC models.

In the next, we focus our attention to the problem of *partial information regulation* to answer the question, how important can be a concrete feedback form. We consider spatially truncated form of feedback defined by energy cumulants calculated for the rectangular $[\phi L] \times L$ lattice segment, where $\phi \in \langle 0, 1 \rangle$ and $[x]$ denotes an integer value of x. The results are depicted in Fig.3b for $L = 60$. The simulation has confirmed that stationary regime is robust with respect to the *partial information regulation* represented by η and $1 - \phi$ terms. As one can be see in Fig.3, both sufficiently small η, $(\eta < \eta_c(L))$, and $1 - \phi$ have similar influence on diminishing the stationary $\langle T \rangle$ value.

As pointed out in Ref. (18), the pdf's of spin clusters at a second-order critical point resembles pdf's of the spatial extent of avalanches. Admittedly, the correspondence between spins and clusters is not unique and thus numerous mapping schemes could be examined. We have utilized the well-known mapping to bond percolation model (19) via Wolf's algorithm (20) to identify cluster without overturning. To interpret the cluster statistics, we suggest the

universal scaling in the form

$$P(s,L) = L^{-\beta}\, g\left(\frac{s}{L^D}\right) , \tag{6}$$

where s is the number of spins belonging to the same cluster. In Fig.4 are depicted spin cluster pdf's. As one can see, the distribution functions for clusters $s \ll s_{\max}(L)$ clearly obey the scaling given by Eq.6, where $s_{\max}(L)$ is proportional to the size of a spanning cluster. It is associated with the peak $P(s_{\max}, L)$ in $P(s,L)$ distribution. Using the scaling relation $s_{\max}(L) \propto L^D$, the fractal dimension $D \simeq 1.98$ has been determined from the fit, see inset in Fig. 4a. Assuming an asymptotic form $g(x) \propto x^{-\tau}$ in the limit $x \to 0$ we obtained $P(s,L) \propto L^{-\beta+\tau D} s^{-\tau}$ that implies independence on L if $\beta = \tau\, D$. Surprisingly, the dependencies in Fig.4b indicate that small-scale power-law scenario survives for full $\eta \in (0,1)$ range. It doesn't matter how distant an assembly is from the thermal equilibrium except a spanning cluster that grows with increasing η.

Since the static bond percolation model pays no attention to temporal variations, the alternative maps should be examined, for instance those taking into account a short-time memory of cluster evolution (21). The question whether differences in a spin - cluster map definition might affect a non-equilibrium exponent β, introduced in Eq.6, is left for future research.

5 The relationship to financial market models

5.1 Statistical properties relevant for financial market modeling

Performed simulations for pdf of F_t defined as $P_{\rm F}(F) \equiv \langle \delta_{F,F_t} \rangle$ confirm that flat tails exhibit within the full range of η, see Fig.5. Therefore, it is worth to check *functional stability* of aggregated regulatory responses

$$r_{n,t} = \sum_{t'=t}^{t+n} F_{t'} \, . \tag{7}$$

The results of analysis depicted in Fig.5b has validated the expected scaling

$$P_{\rm F}(r_n) = r_n^{-1/\alpha}\, f\left(r_n n^{-1/\alpha}\right) \tag{8}$$

for $n < 10$ with estimated exponent $\alpha \simeq 1.3$, where $f(\cdot)$ is some universal function. Since F_t is bounded, the crossing-over from Lévy to Gaussian scaling

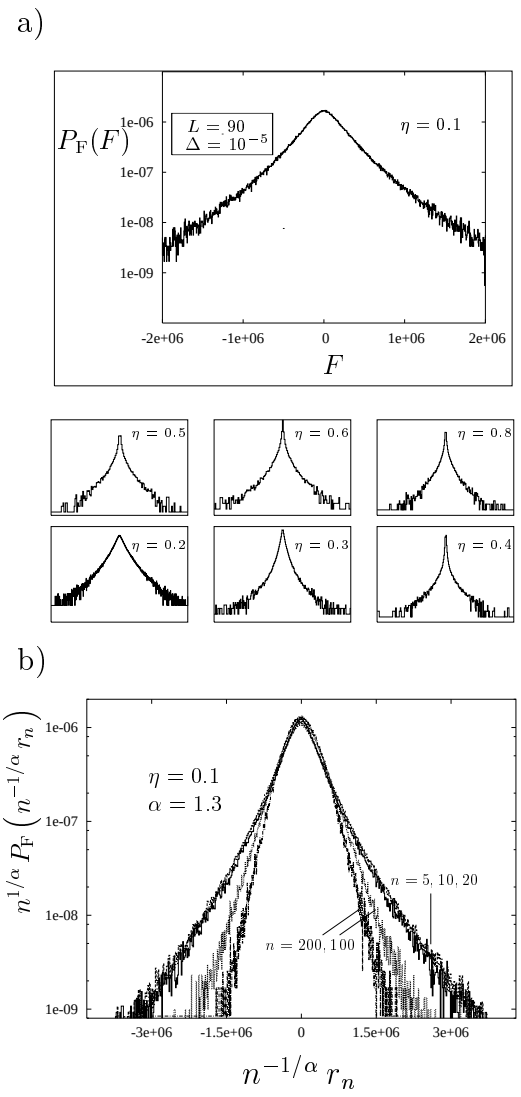

Fig. 5. a) The pdf of F_t shows a high leptocurticity that survive at different choices of η. b) The scaling property given by Eq.(8) and crossing over from the Lévy to Gaussian pdf for $n = 5, 10, 20$. The fluctuations of $r_{n,t}$, $n < 20$ merge to the unique scaling function for $\alpha \simeq 1.3$.

has been verified, see Fig.5b. More profound connection to the price dynamics is discussed in the following section.

The dynamics of self-adjusted system can be analyzed by means of autocorrelation functions of the time lag t:

$$\mathrm{C}_t^{(p)} = \frac{\langle F_{t'}^p\, F_{t'+t}^p \rangle - \langle F_{t'}^p \rangle \langle F_{t'+t}^p \rangle}{\langle (\, F_{t'}\,)^{2p} \rangle - (\langle F_{t'}^p \rangle)^2}\,, \qquad p = 1, 2\,. \tag{9}$$

The MC model yields nearly exponential decrease of $\mathrm{C}_t^{(1)}$, see Fig.6. The power-law dependence of $\mathrm{C}^{(2)}$ which becomes more pronounced for larger L is iden-

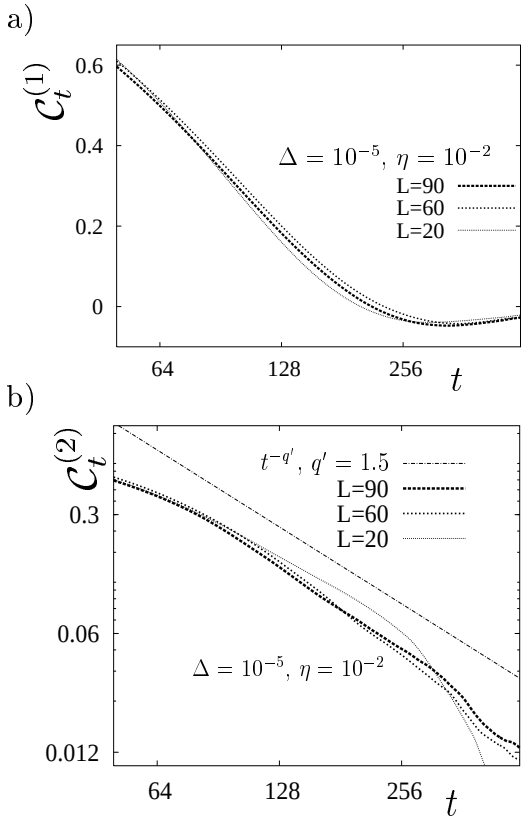

Fig. 6. a) Semilogarithmic logarithmic of autocorrelation function $C_t^{(1)}$ at given interval demonstrate the standard exponential dependence and the long-time anti-correlation zone is also formed. b) Logarithmic plot of the autocorrelation function $C_t^{(2)}$ exhibits power-law regime described by the slope $(-q') = -1.5$. The autocorrelation functions indicate the typical time scale of the order $O(1/\eta^2) = O(100)$.

tified. Assuming the form $C_t^{(2)} \sim t^{-q'}$ we have determined $q' \simeq 1.5$.

5.2 The financial market model formulation

On the basis of previous facts we have proposed model based on the two postulates: (i) under the conditions of new economy the world market entities (participants, companies) are forced to evolve towards the longer auto-correlation times. It means that hardly predicable - volatile price statistics gets stuck in the regime which imply highest degree of uncertainty. It might be classified as an *edge of the chaos*. Such interpretation is fundamentally equivalent with the dynamics of the continuous phase transitions and dynamics of information processing (23); (ii) the centralized institutions are established to satisfy the global information and legislative needs of market entities looking for the arbitrage opportunities. The action of participants leads to enhancement of market effectiveness in the sense of the postulate (i).

Our simulation have shown that presented spin model that involves feedback has much in common with Ising spin market models of the price dynamics (24). The feedback introduced in Bornholdt's model (25), which was later elucidated by Kaizoji, Bornholdt and Fujiwara (BKF), is linked to the local in time and global in lattice space magnetization $m_t = (2/L^2)\sum_{i=1}^{L^2} S_{i,t}$. Both models are inspired by the paradigm of minority game (26). Speaking in game theory term, the feedback promotes the continuing tournaments between competing ordered (ferro) and disordered (para) magnetic phases. To maintain a balance between ordered ferromagnetic and disordered - paramagnetic spin phase, the feedback mechanism including a global cooling or heating is applied. The predicted temperature is simultaneously transmitted to all lattice sites. Clearly, the effect of such step has probabilistic nature, because a freedom exists between the market entities which can uphold or abolish older or establish new coalitions, respectively. Subsequently, any decision is reflected by correlations between entities.

Two principal situations may be observed from the view point of the proposed model. At the subcritical temperatures the clusters grow, which means that correlations among market entities become increase. A subcritical temperature can increase a mean cluster size until a spanning cluster come into existence. The ferromagnetic domain state can be understood as a market situation where competition is distorted due to monopoly, duopoly or trust formation effects. To prevent from highly correlated stocks, the feedback triggers the antitrust operations (27). The portfolio diversification is represented by the fragmentation of the spin clusters.

5.3 The comparison with other spin models of financial markets

The spin model presented in previous sections displays several interesting statistical properties that are particularly relevant for stochastic financial market dynamics. One of our challenges is to examine cross-links between our feedback model and BKF model. In BKF model the local spin behavior is given by the competition between the local and non-local interactions involved in local field $h_{t,i} = 2\,(\sum_{\mathrm{nn}} S_{j,t} - \kappa S_{i,t}|m_t|)$, where κ is proportionality factor of feedback instant magnetization. The probability of $\pm\frac{1}{2}$ lattice spin states is given by $1/[1+\exp(\mp 2\tilde{\beta}h_i)]$, where $\tilde{\beta}$ is the inverse constant temperature. The difference $m_{t+1} - m_t$ is interpreted as a logarithm of the price return. Within the BKF model the instant price is proportional to $\exp(\lambda m_t)$ term, where λ is related to the ratio of the interacting and fundamental traders.

In further we assume the equivalence of $\exp(\lambda m_t)$ and $\exp(\lambda F_t)$ terms considered for different models. The interpretation of $\exp(\lambda F_t)$ as a price term is in accord with requirement that price increases when the competition is

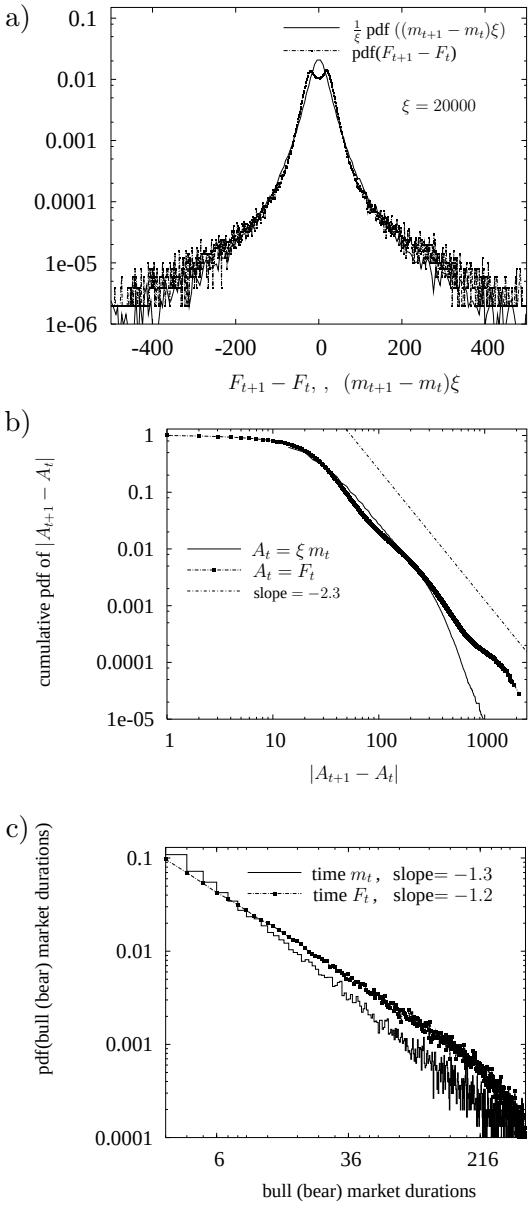

Fig. 7. The comparison of BKF model (solid lines) and model introduced in this paper for the parameters listed in the table 1. a) the rescaling factor ξ is used to attain a full data agreement except the anomaly for small lags $F_{t+1} - F_t$. b) the oscillatory deviations from the power-law has been observed. Despite of this, the rough consistency of cumulative volatility of returns can be attained by rescaling. c) the pdf's of bull (bear) regime durations.

weakened. The crucial items emphasizing the common aspects of models are listed in table 1 and illustrated in Figs. 7 and 8.

We see that both models yield Lévy distributions with the nearly common index $\alpha_1 \sim 3.3$ related to cumulative distributions with power law slope $-2.3 = -\alpha_1 + 1$ that is consistent with the empirical data (29). The bowl-shaped anomaly at small $|F_{t+1} - F_t|$ is probably due to sign(F_t) sharpness. The

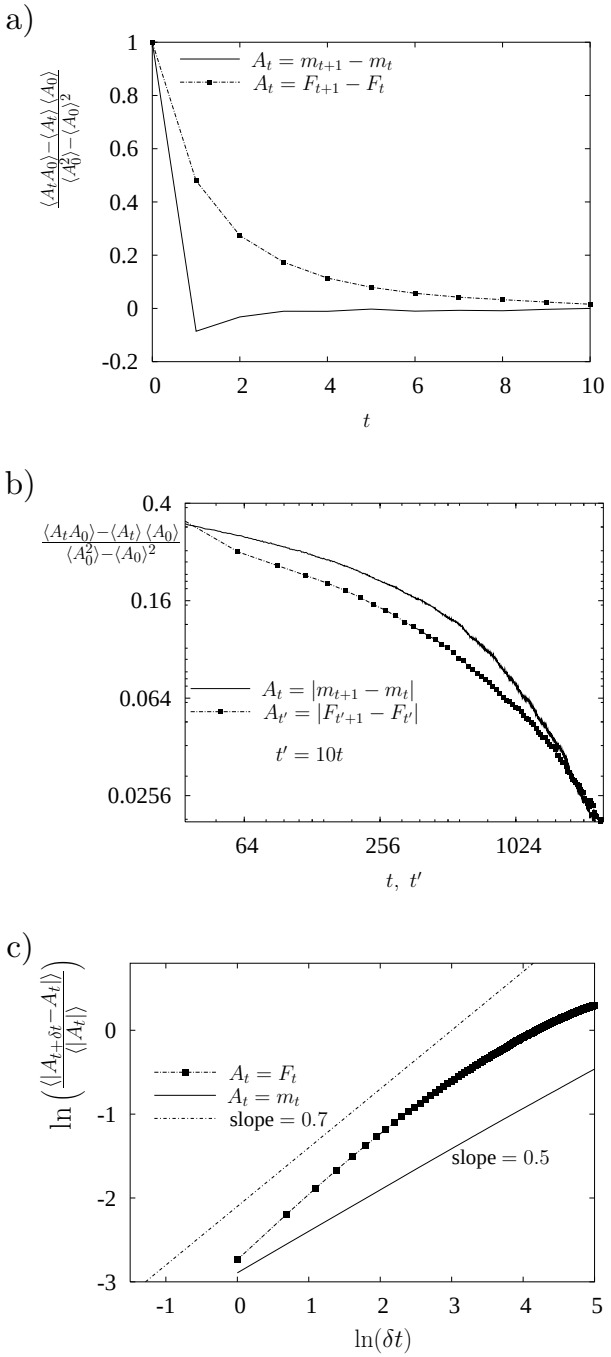

Fig. 8. Comparison for BKF and our model, as in Fig.7, for autocorrelations. a) difference between correlations and anticorrelations as a key distinction. b) volatility autocorrelations with the rescaling $t' = 10\,t$ to emphasize the similarity of models. However, contrary to the expectations in Ref. (28), our fits do not confirmed hypothesis about the power-law volatility autocorrelations in the spin market models. c) principal difference between diffusive (the curve with the slope 0.5 corresponds to BKF) and super-diffusive (slope 0.7) regime.

Table 1
The comparison of the statistical characteristics of models of financial market for $L = 90$. The simulation results obtained for parameters $\eta = 0.01$ and $\Delta = 10^{-5}$. The BKF parameters $\kappa = 20$, $\tilde{\beta} = 2$ are chosen to attain the intermittent regime. The positive F_t (also $m_t > 0$) is the signature of so called bull market regime, while $F_t < 0$ ($m_t < 0$) is interpreted as a bear market regime.

	BKF model	model: sign(F_t)	
price term	$\propto \exp(\lambda m_t)$,	$\propto \exp(\lambda F_t)$	
logarithmic returns	$m_{t+1} - m_t$	$F_{t+1} - F_t$	
pdf of log. returns	leptocurtic	leptocurtic	Fig.7a)
pdf of bull (bear) durations	slope= -1.3	slope= -1.2	Fig.7c)
autocorrelations	anticorrelated	$\exp(-t/1.6)$	Fig.8a)
of logarithmic returns	at $t = 1$	decay	
volatility of log. returns	$\lvert m_{t+1} - m_t \rvert$	$\lvert F_{t+1} - F_t \rvert$	
pdf of volat. log. returns	$\alpha_1 = 3.3$	$\alpha_1 = 3.3$	Fig.7b)
volat. autocorrelations	non-universal	non-universal	Fig.8b)
diffusion of F_t, m_t	diffusion $\delta t^{0.5}$	super-diffusive $\delta t^{0.7}$	Fig.8c)
conditional probabilities			
$\pi(\text{bull}\vert\text{bull})$ $\pi(\text{bull}\vert\text{bear})$	0.978 0.022	0.974 0.026	
$\pi(\text{bear}\vert\text{bull})$ $\pi(\text{bear}\vert\text{bear})$	0.022 0.978	0.026 0.974	

remarkable feature of this comparison is a similarity of the exponents obtained for pdf's of the bull (bear) market durations. In addition, the similarity of temporal aspects can be seen in coincidence of stationary conditional probabilities of bull-bear switching listed in the Table 1. We see that F_t feedback model acquires the exponential form typical for the positively correlated quantities, whereas the magnetization variations predicted by BKF are anticorrelated. Clearly, this difference can be explained providing energy cumulants temporal filtering. The simulation of BKF model reveals some gap between Hurst exponents (30). Contrary to the standard diffusive $\delta t^{0.5}$ behaviour which is typical for $\langle |m_{t+\delta t} - m_t| \rangle$, the superdiffusive short-time regime $\langle |F_{t+\delta t} - F_t| \rangle \sim \delta t^{0.7}$ has been identified for F_t feedback model.

5.4 The application to inter-stock correlations

In the subsection certain diverse application of our model is presented. As one sees, the MC model may be used to understand the basic features of the mechanism of regulation of bilateral stock cross-correlations. The role of cen-

tral institutions, modeled via the feedback, is to perform large-scale eligible decisions that could enhance portfolio efficiency. These contribute to F_t comprising a summary of the stock prices. We assume that different stocks are distinguished by lattice position and sign of dominant trend at given time. And for now the correspondence between spins and stocks follows a simple majority rule: $S_i = \frac{1}{2}$ ($S_i = -\frac{1}{2}$) when the *sell* (buy) market *orders* prevail during elementary time lag (1 MC step/site), respectively. The cross-correlations among directly regulated - four "nearest" stocks are related to the mean exchange energy term $\langle S_i S_{j\in \mathrm{nn}(i)} \rangle$ optimized by F_t to be extremely susceptible to regulation. The long-range cross-correlations stem from indirect regulation of the portfolio composition near to criticality.

The presence of correlations (and anticorrelations) between pairs of stocks play a key role in the theory of selecting of the most efficient portfolio composition of the financial goods (22). For discussed spin model the properties of the pairs of stocks can be characterized by the cross-correlation coefficient

$$c_{ij,t} = \frac{4}{n_{\mathrm{av}}} \sum_{t'=t}^{n_{\mathrm{av}}+t} S_{i,t'} S_{j,t'} \,, \qquad i,j \in \{1,2,\ldots,L^2\} \tag{10}$$

ranging from -1 to 1. Here i, j denote the pair of randomly chosen sites. In the simulations the temporal averages have been calculated for $n_{\mathrm{av}} = 10^3$ steps and accumulated in pdf's depicted in Fig.9. We see that the pair correlations are dominantly positive except a negative tail that agrees qualitatively with the empirical studies (22). For η larger than ~ 0.1 the negative tail vanishes and pdf of $c_{ij,t}$ is shifted towards 1. Clearly, such "coherent" regime is typical for inefficient portfolio structure.

6 Conclusion

In conclusion, we have presented application of adaptivity concept to critical phenomena. Despite of the principal difficulties, insufficient understanding of the systematic errors which arise proceeding from non-equilibrium to equilibrium, we expect that work might inspire numerous applications to other inverse statistical problems where constrains are written in terms of running averages.

We have demonstrated that MC model can be reinterpreted in macro-economic terms. The simulations indicated spontaneous emergence of the power-law distribution for feedback regulatory signals which is universal feature of the stationary non-equilibrium regime. Surprisingly, we found that $F_{t+1} - F_t$ statistics contradicts to our previous expectations based on the finding $\mathrm{C}_t^{(2)} \sim t^{-q'}$,

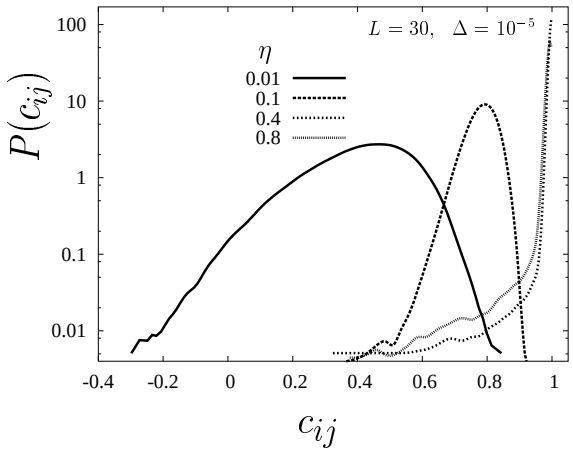

Fig. 9. Cross-correlations distribution obtained for different η [see Eq.(10)]. The anticorrelations appear for $\eta = 0.01$. In that case the distribution can be approximated by double-Gaussian $P(c) = \sum_{k=0,1} w_k \exp[-(c - a_k)^2/(2\sigma_k^2)]$ including the weights $w_0 = 1.432$, $w_1 = 1.951$ and dispersions $\sigma_0 = 0.146$, $\sigma_1 = 0.096$ and $a_0 = 0.337$, $a_1 = 0.493$.

which does not imply power-law fall-off of the autocorrelations of $|F_{t+1} - F_t|$. The influence of the memory depth related to parameter η has also been investigated extensively. The critical point related to the most efficient portfolio structure, is an abstract of ideal situation when $\eta \to 0^+$, which is unattainable in a real finite-memory conditions. Otherwise, we have found that the portfolio efficiency is weakened via short-time memory for $\eta > 0.5$. The comparative study of two spin models have confirmed that presented MC dynamics based on the specific heat feedback offers an alternative description of financial markets. Despite of outstanding similarities, the comparison of exponents indicate non-trivial relationship between the universality classes of studied models.

Acknowledgment

The authors would like to express their thanks to Slovak Grant agency VEGA (grant no.1/2009/05) and agency APVT-51-052702 for financial support.

References

[1] P. Melby, J. Kaidel, N. Weber, A. Hübler, Phys.Rev.Lett. **84** (2000) 5991.

[2] M. Youssefmir, B.A. Huberman, T. Hogg, Computational Economics **12** (1998) 97;
J.A. Holyst, K.Urbanowicz, Physica A **287** (2000) 587.

[3] M.E. Bleich, J.E.S. Socolar, Phys.Rev.E **57** (1996) R16.

[4] D. Horváth, M. Gmitra, Z. Kuscsik, Czech.J.Phys. **54** (2004) 921;

D. Horváth, M. Gmitra, Int.J.Mod.Phys.C. **15** (2004) 1269.
[5] K. Binder, D.W. Heermann, Monte Carlo Simulation in Statistical Physics, Springer, Berlin, 1998.
[6] J.C. Principe, N.R. Euliano, W.C. Lefebvre, Neural and adaptive systems: Fundamentals through simulations, John Wiley & Sons, New York, 2000.
[7] N. Metropolis, A.W. Rosenbluth, M.N. Rosenbluth, A.H. Teller, J.Chem.Phys. **21** (1953) 1087.
[8] P. Buonsante, R. Burioni, D. Cassi, A. Vezzani, Phys.Rev.E **66** (2002) 36121.
[9] P. L. Garrido, A. Labarta, J. Marro, J. Stat. Phys. **49** (1987) 551;
J. M. Gonzales-Miranda, P.L. Garrido, J. Marro, J. L. Lebowitz, Phys.Rev.Lett. **59** (1987) 1934;
K. Basler, Z. Rácz, Phys.Rev.Lett. **73** (1994) 1320.
[10] Y. Tomita, Y. Okabe, Phys. Rev. Lett. **86** (2001) 572.
[11] L. Angelini, Physics Letters A **307** (2003) 41.
[12] L. Onsager, Phys. Rev. **65** (1944) 117;
R.J. Baxter, Exactly Solved Models in Statistical Mechanics, Academic Press, London, 1982.
[13] D.P.Landau, K.Binder, A guide to Monte Carlo simulations in statistical physics, Cambridge University Press, Cambridge, 2000.
[14] P. Bak, C. Tang, K. Wiesenfeld, Phys.Rev.A **38** (1988) 364;
P. Bak, C. Tang, K. Wiesenfeld, Phys.Rev.Lett. **59** (1987) 381;
C. Tang, P. Bak, Phys.Rev.Lett. **60** (1988) 2347.
[15] B. Drossel, F. Schwabl, Phys.Rev.Lett. **69** (1992) 1629.
[16] P. Alstrom, J. Leão, Phys.Rev.Lett. **49** (1994) R2507.
[17] L.P. Kadanoff, Physics Today (March 1991) p. 9
[18] D. Sornete, J. Phys. I France **2** (1992) 2065;
D. Sornette, A. Johansen, I. Dornic, J.Phys. I France **5** (1995) 325.
[19] C.M. Fortuin, P.W. Kasteleyn, Physica **57** (1972) 536.
[20] U. Wolff, Phys. Rev. Lett. **62** (1989) 361.
[21] J.V. Andersen, O.G. Mouritsen, Phys.Rev.A **45** (1992) R5331.
[22] R.N. Mantegna and H.E. Stanley, Introduction to Econophysics: Correlations and Complexity in Finance, Cambridge University Press, Cambridge, 1999.
[23] Ch.G.Langton, "Life at the edge of chaos", p.41 in Artificial life II, Proceedings of the workshop on artificial life held february 1990 in Santa Fe, New Mexico, Proceedings Vol.X, Addison-Wesley, 1990.
[24] A. Ponzi, Y. Aizawa, Physica A **287** (2000) 507;
T. Kaizoji, Physica A **287** (2000) 493;
A. Krawiecki, J.A. Holyst, D. Helbing, Phys. Rev. Letters **89** (2002) 158701;
[25] S. Bornholdt, Int. J. Mod. Phys. C **12** (2001) 667;
T. Kaizoji, S. Bornholdt, Y. Fujiwara, Physica A **316** (2002) 441.
M. Badshah, R. Boyer, T. Theodosopoulos, math.PR/0501244, "*Sta-*

tistical properties of the phase transitions in a spin model for market microstructure", January 2005.

[26] D. Challet, A. Chessa, M. Marsili, Y.-C. Zhang, Quantitative Finance **1** (2001) 168;
D. Challet, Y.-C. Zhang, Physica A **246** (1997) 407;
D. Challet, Y.-C. Zhang, Physica A **256** (1998) 514.

[27] N. Wrigley, Environment and Planning A **24** (1992) 727.

[28] T. Yamano, Int.J.Mod. Phys. C, **13** (2002) 89.

[29] P. Gopikrishnan, V. Plerou, Y. Liu, L.A.N. Amaral, X. Gabaux, H.E. Stanley, Physica A, **287** (2000) 362.

[30] K. Kim, S.M. Yoon, Physica A **344** (2004) 272.